AMERICAN SOCIETY FOR MICROBIOLOGY | Antimicrobial Agents and Chemotherapy®

MECHANISMS OF RESISTANCE

Hydroxylamine and Carboxymethoxylamine Can Inhibit *Toxoplasma gondii* Growth through an Aspartate Aminotransferase-Independent Pathway

Jixu Li,[a] Huanping Guo,[a] Eloiza May Galon,[a] Yang Gao,[a] Seung-Hun Lee,[a,b] Mingming Liu,[a] Yongchang Li,[a] Shengwei Ji,[a] Honglin Jia,[c] Xuenan Xuan[a]

[a]National Research Center for Protozoan Diseases, Obihiro University of Agriculture and Veterinary Medicine, Obihiro, Hokkaido, Japan
[b]College of VeterinaryMedicine, Chungbuk National University, Cheongju, South Korea
[c]State Key Laboratory of Veterinary Biotechnology, Harbin Veterinary Research Institute, Chinese Academy of Agricultural Sciences, Harbin, China

ABSTRACT *Toxoplasma gondii* is an obligate intracellular protozoan parasite and a successful parasitic pathogen in diverse organisms and host cell types. Hydroxylamine (HYD) and carboxymethoxylamine (CAR) have been reported as inhibitors of aspartate aminotransferases (AATs) and interfere with the proliferation in *Plasmodium falciparum*. Therefore, AATs are suggested as drug targets against *Plasmodium*. The *T. gondii* genome encodes only one predicted AAT in both *T. gondii* type I strain RH and type II strain PLK. However, the effects of HYD and CAR, as well as their relationship with AAT, on *T. gondii* remain unclear. In this study, we found that HYD and CAR impaired the lytic cycle of *T. gondii in vitro*, including the inhibition of invasion or reinvasion, intracellular replication, and egress. Importantly, HYD and CAR could control acute toxoplasmosis *in vivo*. Further studies showed that HYD and CAR could inhibit the transamination activity of r*Tg*AAT *in vitro*. However, our results confirmed that deficiency of AAT in both RH and PLK did not reduce the virulence in mice, although the growth ability of the parasites was affected *in vitro*. HYD and CAR could still inhibit the growth of AAT-deficient parasites. These findings indicated that HYD and CAR inhibition of *T. gondii* growth and control of toxoplasmosis can occur in an AAT-independent pathway. Overall, further studies focusing on the elucidation of the mechanism of inhibition are warranted. Our study hints at new substrates of HYD and CAR as potential drug targets to inhibit *T. gondii* growth.

KEYWORDS *Toxoplasma gondii*, toxoplasmosis, hydroxylamine, carboxymethoxylamine, aspartate aminotransferase

The phylum *Apicomplexa* comprises a grand group of intracellular parasites that have been implicated in many important human and veterinary diseases. *Plasmodium* spp. and *Toxoplasma gondii* are the most representative and best studied members of this large phylum (1). *T. gondii* is an obligate intracellular protozoan parasite which can infect warm-blooded animals, including humans (2). The majority of the isolates from North America and Europe belong to one of three distinct lineages based on the laboratory mouse model: acutely virulent type I, intermediate type II, and avirulent type III strains (3–5). *T. gondii* causes toxoplasmosis, and one-third of the world's population is estimated to be infected with this parasite (6), but the infection is usually asymptomatic in immunocompetent individuals, whereas immunocompromised people may present with acute toxoplasmosis or even with severe and even fatal complications. Unfortunately, although the gold-standard treatment of toxoplasmosis uses a combination of sulfonamide and pyrimethamine drugs (7), treatments for *T. gondii* infections are suboptimal (8, 9), since synergistic activity could only be observed against

Citation Li J, Guo H, Galon EM, Gao Y, Lee S-H, Liu M, Li Y, Ji S, Jia H, Xuan X. 2020. Hydroxylamine and carboxymethoxylamine can inhibit *Toxoplasma gondii* growth through an aspartate aminotransferase-independent pathway. Antimicrob Agents Chemother 64:e01889-19. https://doi.org/10.1128/AAC.01889-19.

Address correspondence to Honglin Jia, jiahonglin@caas.cn, or Xuenan Xuan, gen@obihiro.ac.jp.

Received 17 September 2019
Returned for modification 17 November 2019
Accepted 23 December 2019
Accepted manuscript posted online 6 January 2020
Published 21 February 2020

tachyzoites and not against bradyzoites, and severe side effects and adverse drug reaction have been reported.

The *T. gondii* lytic cycle develops beginning with extracellular energy-dependent tachyzoite invasion into host cells, followed by rapid intracellular tachyzoite replication, egress, and reinvasion of neighboring cells (10). In these stages, not only glucose but also glutamine can enter the mitochondria as a carbon source (10–14), where glutamine can be utilized as carbon skeletons to the tricarboxylic acid (TCA) cycle via either the conversion of intermediate glutamate to α-ketoglutarate or the γ-aminobutyric acid (GABA) shunt (13). The *T. gondii* genome contains enzymes allowing speculation on a possible architecture of α-ketoglutarate pathway (1), which includes an aspartate aminotransferase (AAT). AAT, as metabolic enzyme, catalyzes the reversible conversion of oxaloacetate and glutamate into aspartate and α-ketoglutarate and subsequently α-ketoglutarate as an intermediate can enter the TCA cycle used for *T. gondii* proliferation (1). Metabolic enzymes play crucial roles not only in parasite proliferation but also in pathogenicity, which contributes to the virulence of parasites in mouse models and used as potential drug targets (13, 15–18).

Previous studies demonstrated that AAT of *Plasmodium falciparum* catalyzes the reversible reaction of aspartate and α-ketoglutarate to glutamate (1, 19, 20); these are important intermediates for developing carbon metabolism and the amino acid cycle for parasite survival. Hydroxylamine (HYD) and carboxymethoxylamine (CAR) are inhibitors of AATs, abolish the transamination activity of *Pf*AAT, and interfere with the proliferation of the parasite (19–22). Therefore, *Pf*AAT is believed to be a promising drug target.

Here, we analyzed AAT of *T. gondii* and evaluated the anti-*T. gondii* potential of HYD and CAR *in vitro* and *in vivo*. Our data indicated that HYD and CAR may be useful for treating toxoplasmosis and even acute *T. gondii* infection through an AAT-independent pathway.

RESULTS

HYD and CAR inhibit *T. gondii* growth *in vitro*. First, we analyzed the toxicity of HYD and CAR on host cells *in vitro* using a CCK-8 cell counting kit. When human foreskin fibroblast (HFF) cells were exposed to 100 μg/ml HYD for 24 h, the cell proliferation rate was 109.02%; when the cells were exposed to 200 μg/ml HYD, the proliferation rate fell to 54.51% (Fig. 1A). The cytotoxic 50% inhibitory concentration (IC_{50}) value was determined to be 210.2 μg/ml (Fig. 1B). However, when HFF cells were treated with CAR, even at high concentrations of 1,000 μg/ml, the proliferation rate was $>$95.89% (Fig. 1A). Therefore, the safe concentrations of compounds for HFF cells were considered to be $<$100 μg/ml for HYD and 1,000 μg/ml for CAR in this study. For monkey kidney adherent epithelial (Vero) cells exposed to 200 μg/ml HYD the proliferation rate was 101.11%, while for Vero cells exposed to 400 μg/ml the proliferation rate was only 6.94% (Fig. 1C). The IC_{50} value of HYD against Vero cells was 296.6 μg/ml (Fig. 1D). A proliferation rate of 97.78% was noted on Vero cells treated with 1,000 μg/ml CAR (Fig. 1C). Therefore, the safe concentrations of compounds for Vero cells were considered to be $<$200 μg/ml HYD and 1,000 μg/ml CAR in this study.

To evaluate the potential of anti-*Toxoplasma* of compounds *in vitro*, we examined the fluorescence intensity of RH-GFP on HFF cells after treatment with HYD, CAR, dimethyl sulfoxide (DMSO; negative control), and sulfadiazine (positive control). RH-GFP parasite growth was inhibited by 50 μg/ml CAR with little fluorescence (see Fig. S1 in the supplemental material), while the green fluorescent protein (GFP) signal was still detected, even at the highest concentration of sulfadiazine (1 mg/ml). Both compounds were able to inhibit parasite growth, with IC_{50} values of 4.286 μg/ml for HYD and 23.11 μg/ml for CAR on RH-GFP (Fig. 1E and F). Meanwhile, the selectivity indices for HYD and CAR for RH-GFP on HFF cells were 49.04 and $>$43.27, respectively.

The *T. gondii* lytic cycle is impaired by HYD and CAR *in vitro*. *T. gondii* lytic cycle starts from the energy-dependent extracellular tachyzoite invasion into host cells, followed by rapid intracellular tachyzoite replication, egress, and reinvasion of neigh-

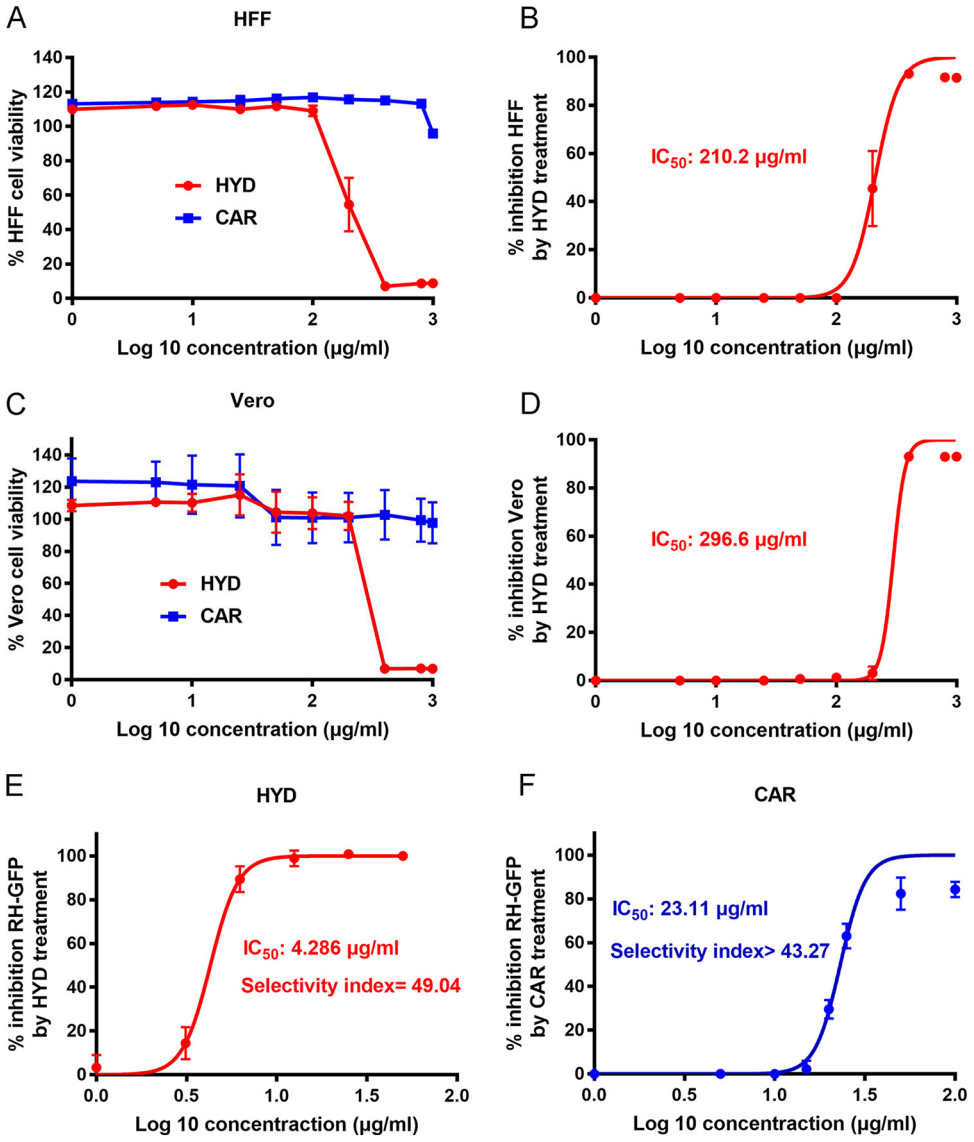

FIG 1 HYD and CAR were able to inhibit parasite growth. (A) HFF cell viability upon treatment with HYD and CAR. (B) Inhibition of HFF growth with HYD treatment. The 50% inhibitory concentration (IC_{50}) was examined. (C) Vero cell viability upon treatment with HYD and CAR. (D) Inhibition of Vero cell growth by HYD treatment. (E and F) Inhibition of *T. gondii* type I parasites (RH-GFP) after HYD (E) and CAR (F) treatment. The IC_{50} and selectivity index values were determined.

boring cells (10). Studies on plaque formation can result the complete rounds of *T. gondii* lytic cycle *in vitro* (23, 24). Therefore, to analyze the effects of HYD and CAR on the lytic cycle of *T. gondii*, 2- or 4-fold IC_{50} values for either of the compounds were used to perform attachment and invasion, replication, and egress assays on Vero cells; also, 2-fold IC_{50} values for compounds were used to conduct plaque formation assays on HFF cells.

For parasite invasion, 2-fold IC_{50} values for HYD or CAR decreased the percentages of invaded parasites, although not significantly. Remarkably, when treated by 4-fold IC_{50} values, the invasion was significantly reduced by 46.03% for HYD and 43.36% for CAR, whereas only a 12.41% reduction in tachyzoite invasion was determined upon treatment with even a high concentration of sulfadiazine (1 mg/ml) (Fig. 2A).

To determine the effects of HYD and CAR on intracellular replication *in vitro*, Vero cells were infected with fresh tachyzoites for 24 h in the presence of 2- or 4-fold IC_{50} values for either of the compounds and 1 mg/ml sulfadiazine. Parasite replication was

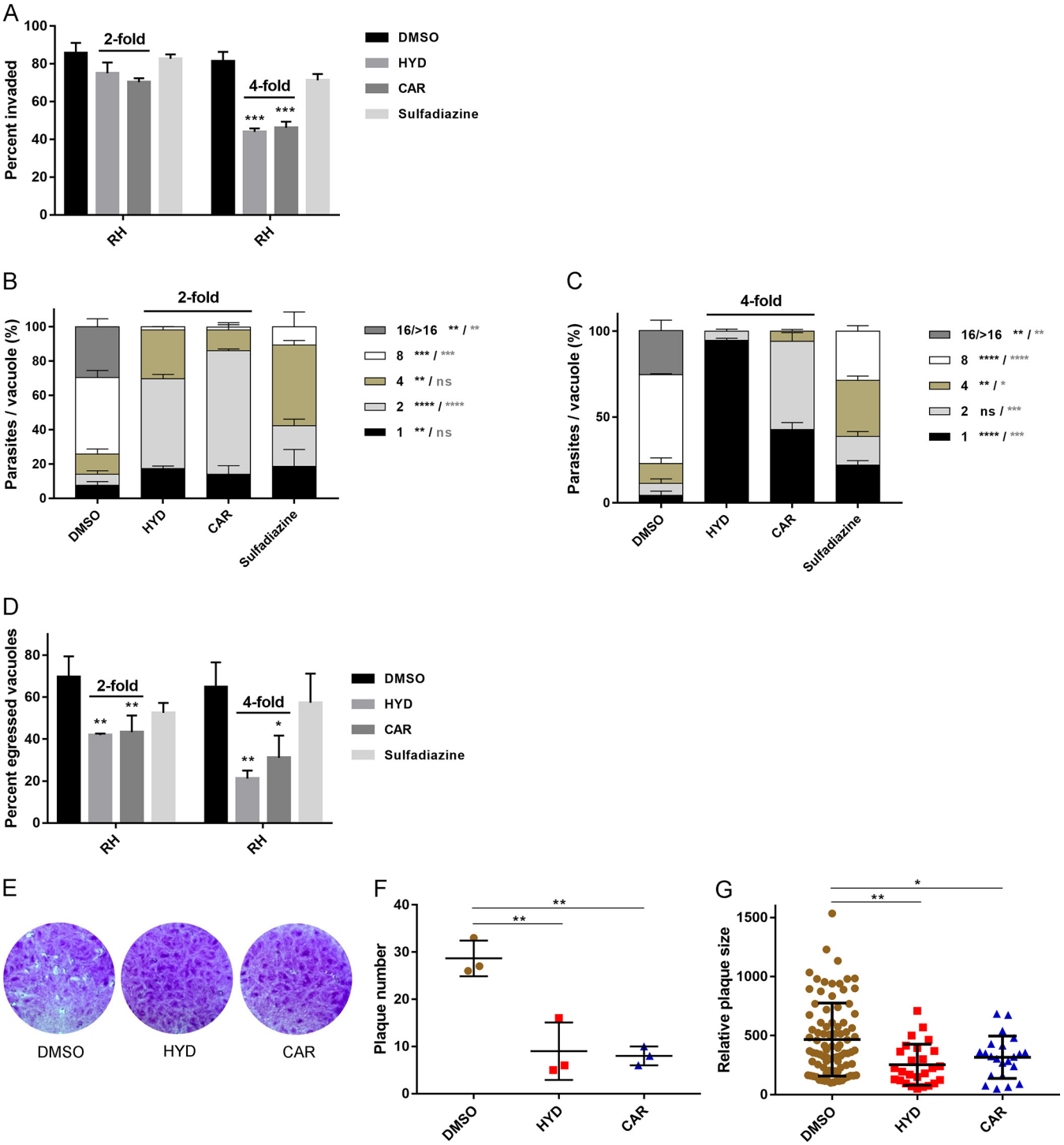

FIG 2 *T. gondii* lytic cycle is impaired by HYD and CAR *in vitro*. (A) Invasion assay. Purified tachyzoites were pretreated with either of the two compounds of 2- or 4-fold IC_{50} values, sulfadiazine (1 mg/ml), or DMSO for 1 h at 37°C, followed by invasion for 2 h, and dual staining was used to determine the percentages of invaded parasites. (B and C) Intracellular replication assay. HYD and CAR 2-fold (B) or 4-fold (C) IC_{50} values were allowed to treat infected RH parasites for 24 h, and the numbers of parasites in 100 random vacuoles were counted and plotted. (D) Egress assay. Infected cells were treated with compounds at 2- and 4-fold IC_{50}s for 10 min before incubation with 3 μM A23187. After incubation, mouse anti-SAG1 and rabbit anti-GRA7 were used to measure the percentage of staining egressed PVs. At least 300 vacuoles were counted per slip. (E) Plaque formation assay. A total of 150 fresh RH strain tachyzoites were used to infect the HFF cell monolayer and allowed to grow for 8 days with HYD or CAR at an 2-fold IC_{50} value, and then 0.1% crystal violet was used for staining. (F and G) Relative plaque numbers (F) and plaque sizes (G) from panel D. The data are presented as the means ± the SEM of at least three independent experiments. *, $P < 0.05$; **, $P < 0.01$; ***, $P < 0.001$; ****, $P < 0.0001$ compared to DMSO treatment, determined by chi-square test (invasion and egress assay), Tukey's multiple-comparison test (replication assay, a heavy asterisk represents HYD versus vehicle, and a light asterisk represents CAR versus vehicle), and one-way ANOVA plus Tukey-Kramer *post hoc* analysis (plaque assay).

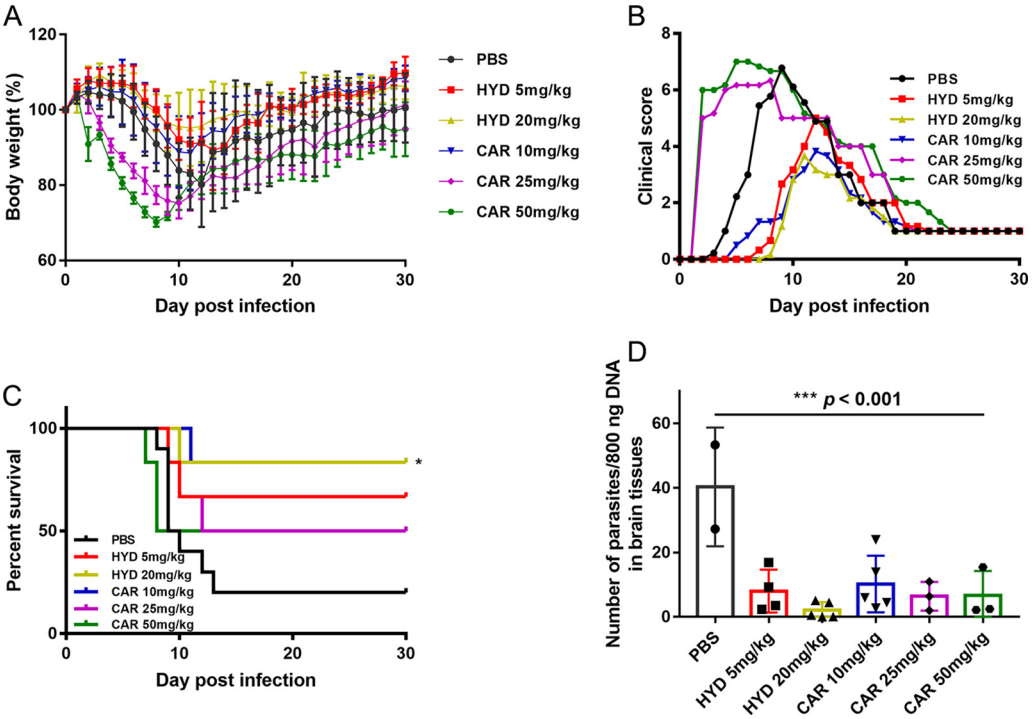

FIG 3 HYD and CAR control acute *Toxoplasma* infection in mice. Female BALB/c mice were infected i.p. with an acute dose of 50,000 PLK tachyzoites and treated i.p. from day 1 to day 7 postinfection with 5 or 20 mg/kg HYD; 10, 25, or 50 mg/kg CAR; or PBS once daily. The body weight, morbidity, mortality, and clinical signs were noted. (A) Body weight (%). (B) Mean clinical scores. The scores varied from 0 (no signs) to 10 (all signs). (C) Survival rates. *, $P < 0.05$, log-rank (Mantel-Cox) test. (D) Parasite burdens of survival mice brains. At day 30 postinfection, the brains were collected, and DNA was extracted, 800 ng of DNA was used to detect the number of parasites. ***, $P < 0.001$, one-way ANOVA plus Tukey-Kramer *post hoc* analysis.

impaired upon treatment with 2-fold IC_{50} values of HYD or CAR, and replication was almost completely abolished by treatment with 4-fold IC_{50} values of these compounds (Fig. 2B and C). Notably, HYD showed a stronger inhibitory effect than did CAR. For the egress assay, both HYD and CAR pretreatment significantly decreased the egress rate compared to DMSO pretreatment (Fig. 2D), suggesting that tachyzoite egress from host cells was impaired.

We conducted a plaque assay to observe the complete round of the lytic cycle (Fig. 2E). In the presence of HYD or CAR, parasites formed smaller plaques with lower plaque numbers than those in DMSO treatment experiments (Fig. 2F and G). These results suggest that the *T. gondii* lytic cycle is impaired by HYD and CAR *in vitro*.

Treatment with HYD and CAR controls acute toxoplasmosis in mice. To evaluate the effects of compounds on *T. gondii in vivo*, female BALB/c mice were infected intraperitoneally (i.p.) with an acute dose of 5×10^4 type II PLK strain tachyzoites and treated by i.p. with 5 or 20 mg/kg (body weight) HYD; 10, 25, or 50 mg/kg (body weight) CAR; or phosphate-buffered saline (PBS) once daily from days 1 to 7 postinfection. Body weight, morbidity, mortality, and clinical signs were recorded. As expected, treatment with 20 mg/kg HYD and 10 mg/kg CAR significantly increased the survival rate during acute infection, with slight body weight reduction and lower clinical scores, compared to PBS treatment (Fig. 3A to C). However, the higher clinical scores were seen in the 25- and 50-mg/kg CAR-injected mice beginning 2 days postinfection (dpi). Moreover, 50 mg/kg CAR-treated mice died at 7 and 8 dpi, earlier than PBS-treated mice, suggesting that although CAR can control acute toxoplasmosis, high concentrations can be toxic to mice. On the other hand, the parasite burdens in surviving mouse brain tissues were examined by quantitative PCR (qPCR), and we observed significantly lower loads in HYD- and CAR-treated mouse brains than in PBS-treated mice (Fig. 3D). Collectively,

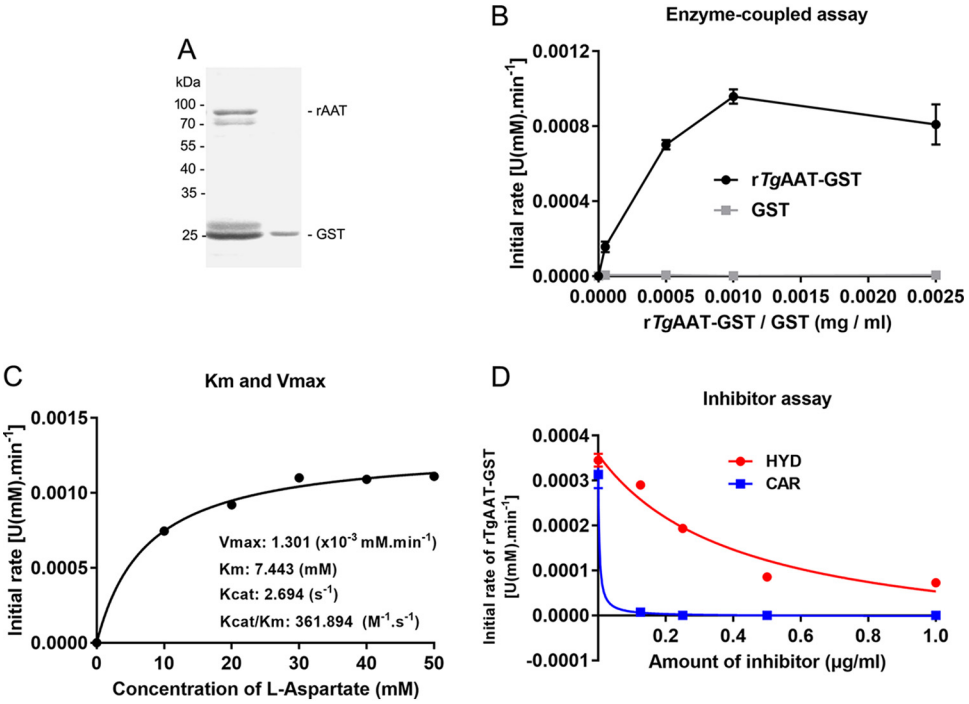

FIG 4 HYD and CAR impair r*Tg*AAT catalytic activity. (A) Soluble r*Tg*RHAAT expression. The concentration of soluble r*Tg*AAT-fused GST was determined. (B) Generation of an enzyme-coupled assay. Expressed GST was used as a control. (C) Enzyme reaction. The enzyme activities of catalysis aspartate and α-ketoglutarate into glutamate were determined using 1 μg of r*Tg*AAT. (D) Inhibitor assay. The enzyme reaction was inhibited with increasing amounts of HYD and CAR.

HYD and CAR treatment controlled acute *Toxoplasma* infection in the mouse model, although some parasites were detected in the brain samples.

HYD and CAR inhibit the catalytic reaction of r*Tg*AAT. To analyze whether also HYD and CAR can inhibit enzymatic transamination activity of r*Tg*AAT protein as in *P. falciparum* (19), we cloned and sequenced the gene encoding *Tg*AAT from the *T. gondii* type I RH and type II PLK strains, indicating *Tg*AATs coding sequences were 1,794 bp long, which is consistent with the predicted sequence (ToxoDB TGGT1_248600 and TGME49_248600), and soluble r*Tg*RHAAT was expressed (Fig. 4A) and used to perform an enzyme-coupled assay, as described previously (19). Soluble r*Tg*AAT (1 μg) was used to conduct enzyme reaction with the specific substrate L-aspartate. We demonstrated that L-aspartate is the preferred substrate of r*Tg*AAT, with a specific activity of 0.078 ± 0.12 μmol min^{-1} mg^{-1} (Fig. 4B and C). As expected, the reaction of 1 μg of r*Tg*AAT was inhibited by HYD and CAR treatment, with IC_{50}s of 0.4158 and 0.0035 μg/ml, respectively (Fig. 4D).

Knockout *Tg*AAT on RH and PLK strains. First, for the *Tg*AAT sequence, the amino acid sequence alignment was analyzed, and the phylogenetic tree was constructed with AATs from other species, including *Homo sapiens* (AAC28622.1), *Mus musculus* (NP_034454.2), *Plasmodium falciparum* (KNG76684.1), *Eimeria tenella* (XP_013230025.1), *Trypanosoma brucei* (AAK73815.1), *Giardia intestinalis* (AAK73817.1), and *Escherichia coli* (AHG10759.1) (see Fig. S2A in the supplemental material). It revealed that *Tg*AATs were distantly related to the predicted *P. falciparum*, with 33% identity. Western blot analysis revealed that the expression levels of native AAT proteins in RH and PLK strains were not significantly different (Fig. S2B and C), suggesting that *Tg*AAT may play a similar role in both strains.

To investigate further the HYD and CAR target of AAT in *T. gondii*, we proceeded to generate two knockout strains (Δ*RHaat* and Δ*PLKaat*) using pDF-Cas9-sgAAT plasmid (Fig. S2D) and two complemented strains (ComRHAAT and ComPLKAAT strains) using

pB-synoRHAAT or pB-synoPLKAAT plasmids (Fig. S2E) containing codons synonymous to *Tg*AATs by CRISPR/Cas9-mediated genome editing. Diagnostic PCRs were used to screen single clones and to confirm gene deletions and complements. The AAT and uracil phosphoribosyl transferase (UPRT) genomic fragments were not amplified in knockout (Fig. S2F) and complemented (Fig. S2G) parasites, whereas the different fragments within plasmids were amplified. After selection, Δ*RHaat*, Δ*PLKaat*, ComRHAAT, ComPLKAAT, and wild-type strains were all verified by Western blotting (Fig. S2H). Protein bands were observed in the lysates of RH/PLK and ComRH/PLKAAT lines using a specific anti-*Tg*AAT antibody, but not in the knockout strains. An indirect fluorescent antibody test (IFAT) demonstrated that *Tg*AAT was expressed in the wild-type and complemented parasites but not in the mutant strains (Fig. S2I). These data confirmed the loss of AAT in both RH and PLK strains and the homologous integration and insertion of synoAAT at the UPRT site in representative complement.

Disruption of *Tg*AAT on RH and PLK strains slows parasite growth *in vitro*. To estimate the impact of AAT disruption on parasite growth *in vitro*, all strains were used to determine the production of plaques on Vero cell monolayers. The results showed that all strains are able to form plaques (Fig. 5A and C). Significantly smaller of plaque sizes were present in Δ*PLKaat* parasites compared to PLK parasites, whereas the plaques of Δ*RHaat* and RH parasites showed no significant differences (Fig. 5B and D).

To better define the phenotype associated with the loss of AAT, the effect in invasion, intracellular replication, and egress was evaluated *in vitro* and compared to parental parasite growth under standard tachyzoite growth conditions. As shown in Fig. 5E, the deletion of AAT in the RH strain significantly inhibited the parasite's invasion, replication, and egress abilities *in vitro*. Similar results were evident in the loss of AAT in PLK (Fig. 5F). These results show that AAT is dispensable for the intracellular growth of parasites but that the ability of parasites to spread *in vitro* is significantly impaired after the deletion of AAT in both RH and PLK strains.

Treatment with α-ketoglutarate rescues the growth defect in AAT deletion mutants. *Tg*AAT catalyzes glutamate into α-ketoglutarate, an important intermediate of carbon metabolism in mitochondria. To investigate whether α-ketoglutarate supplementation can rescue the growth defect in AAT deletion parasites, the levels of intracellular replication under different culture conditions were compared. The results showed that α-ketoglutarate supplementation (400 μM) significantly increased the 24-h replication rates in AAT-deficient parasites of the RH strain (Fig. 6A) and the PLK strain (Fig. 6B). A lack of more profound improvement by α-ketoglutarate may be due to poor uptake of this nutrient. Indeed, we also examined plaque formation, which resulted in the AAT deletion PLK mutant forming significantly larger plaques in the presence of exogenous α-ketoglutarate (Fig. 6C and D). Interestingly, the high concentration of α-ketoglutarate (2 mM) led to faster intracellular replication of AAT-deficient parasites compared to parental PLK *in vitro* (Fig. 6E). Taken together, the rescue of AAT-deleted mutants by α-ketoglutarate suggests that AAT plays an important role during *T. gondii* nutrient uptake.

Loss of *Tg*AAT in PLK strain does not abolish the virulence of parasites *in vivo*. To assess the degree of virulence of Δ*aat* mutants, mice were infected with increasing doses of tachyzoites (10,000, 30,000, or 50,000 parasites per mouse [PLK group] and 100 parasites per mouse [RH group]). At an infection dose of 100 tachyzoites per mouse, RH, Δ*RHaat*, and ComRHAAT parasites caused all 100% mortality within 9 dpi in animals with similar body weights (%) (Fig. 7A and B) and no differently acute symptoms (data not show). An infection dose of 1×10^4 PLK group tachyzoites was not fatal, whereas a dose of 3×10^4 or 5×10^4 Δ*PLKaat* parasites caused 100% mortality with a significant reduction in body weight (Fig. 7C and D). This virulence was even greater than that observed for wild-type PLK and ComPLKAAT parasites.

HYD and CAR inhibit *T. gondii* growth by an AAT-independent pathway. The aforementioned results show that HYD and CAR control acute *T. gondii* infection in mice; however, AAT deficiency does not abolish the virulence of PLK or RH *in vivo*.

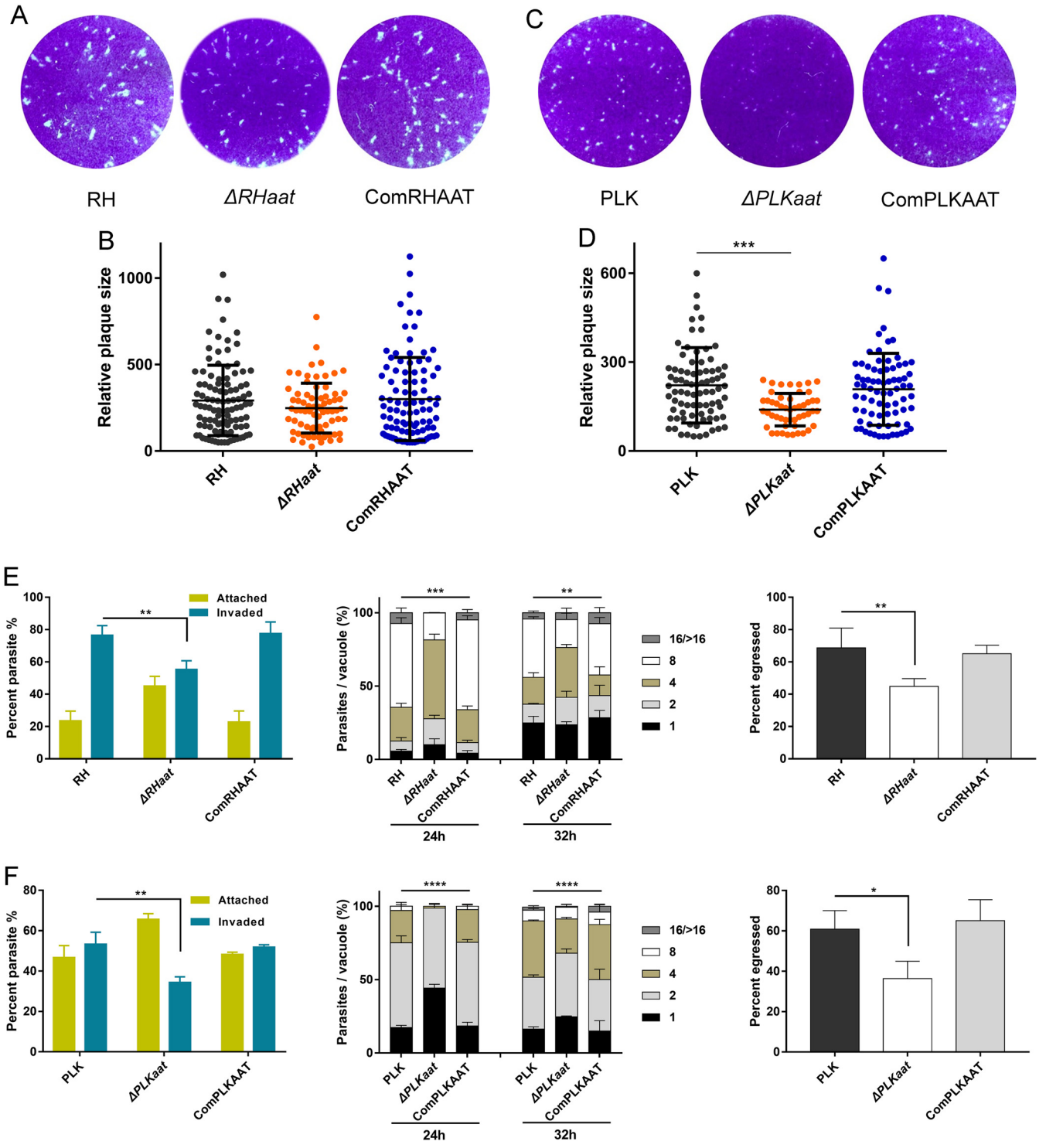

FIG 5 AAT deficiency slows down RH and PLK parasite growth *in vitro*. (A) Plaque assay. The growth of 150 Δ*aat* or ComAAT tachyzoites *in vitro* was compared to that of parental RH strains. Plaques were visualized by staining with 0.1% crystal violet. (B) Relative size of the plaques in panel A. The data are presented as means ± the SEM of three independent experiments. (C) Plaque formation of the Δ*PLKaat* tachyzoites *in vitro*. Vero cells were infected by 300 tachyzoites and cultured for 12 days. (D) Relative size of plaques in panel C. The data are presented as means ± the SEM of three independent experiments. ***, $P < 0.001$, one-way ANOVA plus Tukey-Kramer *post hoc* analysis. (E and F) Invasion, replication, and egress assays of mutants compared to parental and complemented strains in RH (E) and PLK (F) lines. The data are presented as means ± the SEM of at least three independent experiments. *, $P < 0.05$; **, $P < 0.01$; ***, $P < 0.001$; ****, $P < 0.0001$, determined by chi-square test (invasion and egress assay) and Tukey's multiple-comparison test (replication assay).

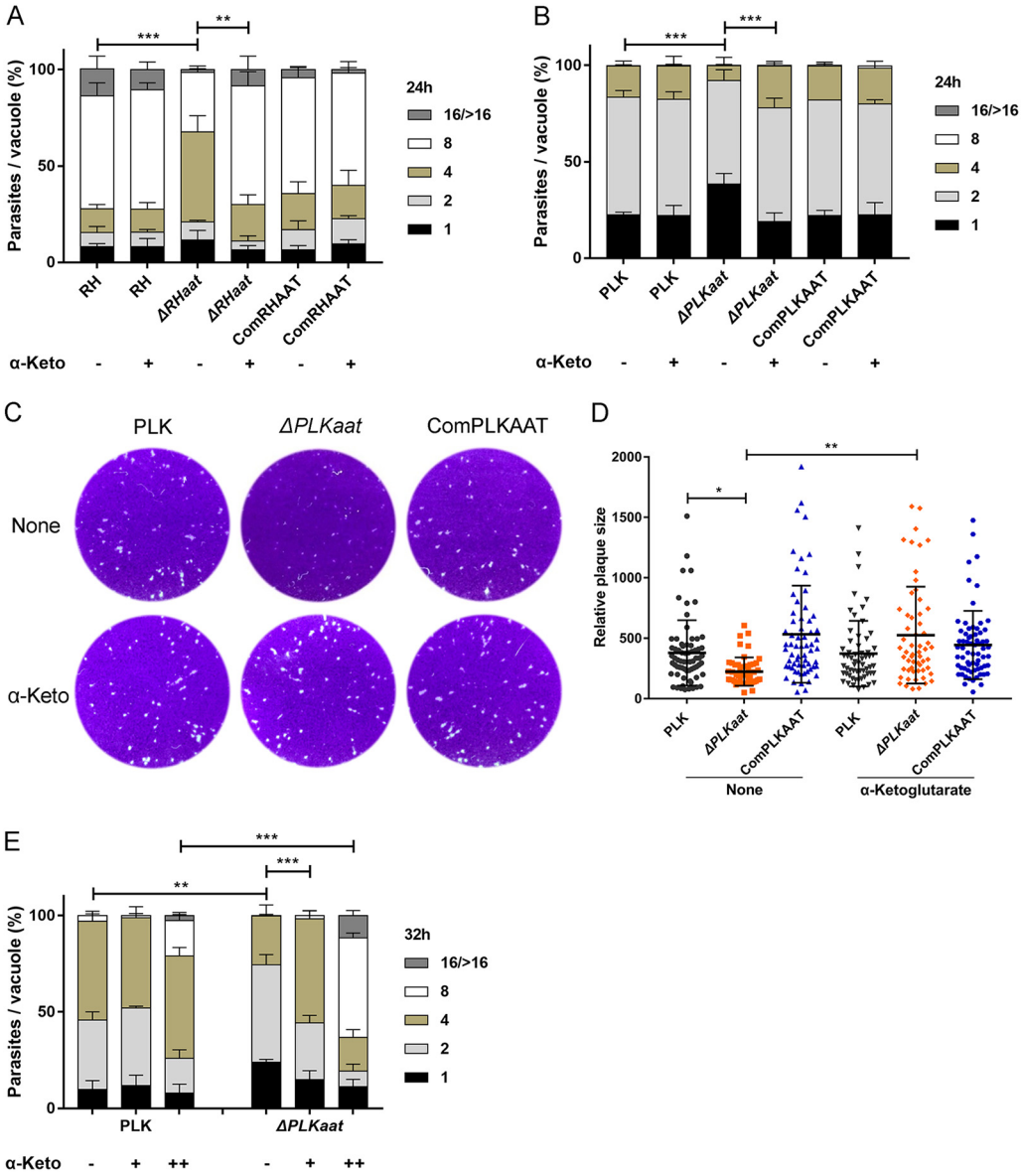

FIG 6 Supplementation with α-ketoglutarate (α-Keto) rescues growth defects in Δ*aat* tachyzoites. (A) Supplementation assay with α-ketoglutarate (400 μM) on type 1 strain RH. Tachyzoites were grown with or without α-ketoglutarate 24 h postinfection, and the numbers of parasites in each PV were then determined. (B) PLK replication rescued by α-ketoglutarate (400 μM). Infected tachyzoites were cultured in Vero cells with or without α-ketoglutarate for 24 h, and then the numbers of parasites in each PV were determined. (C) Plaque formation of Δ*PLKaat* tachyzoites under α-ketoglutarate supplementation conditions. (D) Relative size of plaques in panel C. (E) The high concentration of α-ketoglutarate (2 mM) led to faster replication of AAT-deficient parasites compared to parental PLK *in vitro*. The data are presented as means ± the SEM of three independent experiments. –, no treatment with α-ketoglutarate; +, treatment by a low concentration (400 μM); ++, treatment by high a concentration (2 mM). *, $P < 0.05$; **, $P < 0.01$; ***, $P < 0.001$, one-way ANOVA plus Dunnett's multiple-comparison test (replication assay) and one-way ANOVA plus Tukey-Kramer *post hoc* analysis (plaque assay).

Therefore, HYD and CAR might inhibit *T. gondii* growth through AAT-independent pathway. To evaluate this possibility, AAT deletion parasites were treated with either HYD or CAR to determine the effects on extracellular invasion and intracellular replication. The results showed that treatment with as high as 4-fold IC_{50} values of HYD and CAR yielded invasion rates of mutant parasites that were not significantly different among the HYD, CAR, and DMSO treatment groups compared to the wild-type and complemented invasion rates (Fig. 8A and B). Interestingly, as presumed above, intracellular replication of AAT-deficient parasites was also slowed down by both 2- and

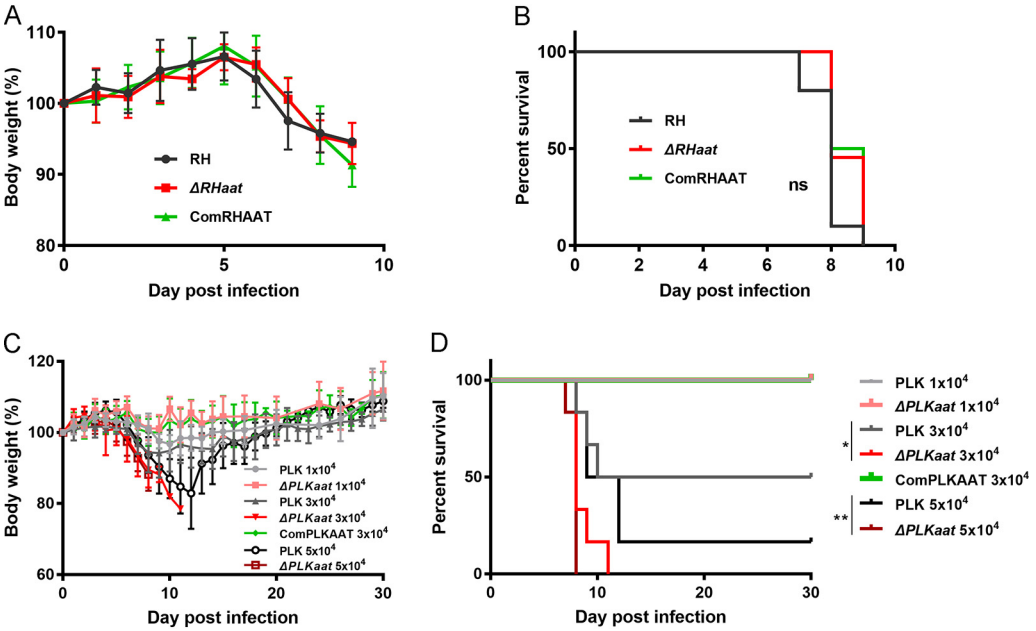

FIG 7 Virulence tests of Δ*aat* tachyzoites in mice. (A and B) Body weight (%) (A) and survival rate (B) during Δ*RHaat* infection. Mice were infected by i.p. injection with 100 RH ($n = 11$), Δ*RHaat* ($n = 11$), or ComRHAAT ($n = 6$) tachyzoites. (C) Body weight during Δ*PLKaat* infection. Six mice were infected with 10,000, 30,000, and 50,000 tachyzoites by i.p. injection. (D) Survival rate of PLK AAT deficiency parasite infection in mice. Survival curves of mice infected with Δ*PLKaat* tachyzoites were noted until day 30. *, $P < 0.05$; **, $P < 0.01$, log-rank (Mantel-Cox) test.

4-fold IC_{50}s of HYD and CAR compared to parental parasites (Fig. 8C). On the other hand, the results showed that α-ketoglutarate supplementation significantly rescued defects due to loss of AAT, so we also sought to determine whether HYD- or CAR-impaired growth can be rescued by α-ketoglutarate. Our experiments revealed that the presence of α-ketoglutarate in HYD- or CAR-treated RH-infected cells slightly increased parasite replication (Fig. 8D). Altogether, HYD and CAR inhibit *T. gondii* growth in a way that is largely independent of the AAT pathway. Further, the use of a 0.25-, 0.5-, or 1-fold IC_{50} of HYD and CAR to treat RH parasite growth for 5 days showed that the relative transcription levels of mitochondrial genome (CytB gene) were reduced by increasing the compound concentrations (Fig. 8E), suggesting that compounds impairing the parasite lytic cycle may be related to mitochondrial function.

DISCUSSION

Our studies reveal that HYD and CAR inhibited *T. gondii* growth by impairing the rounds of the lytic cycle, including inactivated extracellular invasion or reinvasion, slowed intracellular replication, and inhibited egress resulting in unformed plaques. Importantly, HYD and CAR also showed anti-*Toxoplasma* activity *in vivo*. As for the inhibition of asexual stages, it is not surprising that acute infection of *T. gondii* was controlled by both compounds in mice.

A previous study reported that the parasitic IC_{50} value of sulfadiazine anti-*T. gondii* type I parasites (RH strain) on HFF cells was 70 μg/ml (25), whereas in the present study lower IC_{50} values of HYD and CAR on type I RH-GFP strain in HFF cells (4.286 and 23.11 μg/ml, respectively) were obtained. Regarding pyrimethamine, we did not test the effects in this study due to the currently used RH-GFP parasites, which have the pyrimethamine-resistant gene (DHFR) (26–28). However, a published study reveals that an IC_{50} value of pyrimethamine against *T. gondii* of 0.84 μg/ml and a selectivity index (SI) value of $>$11.9 (29). The obtained IC_{50}s of HYD and CAR on type I strain (RH-GFP) are between the values for sulfadiazine and pyrimethamine, and the current results

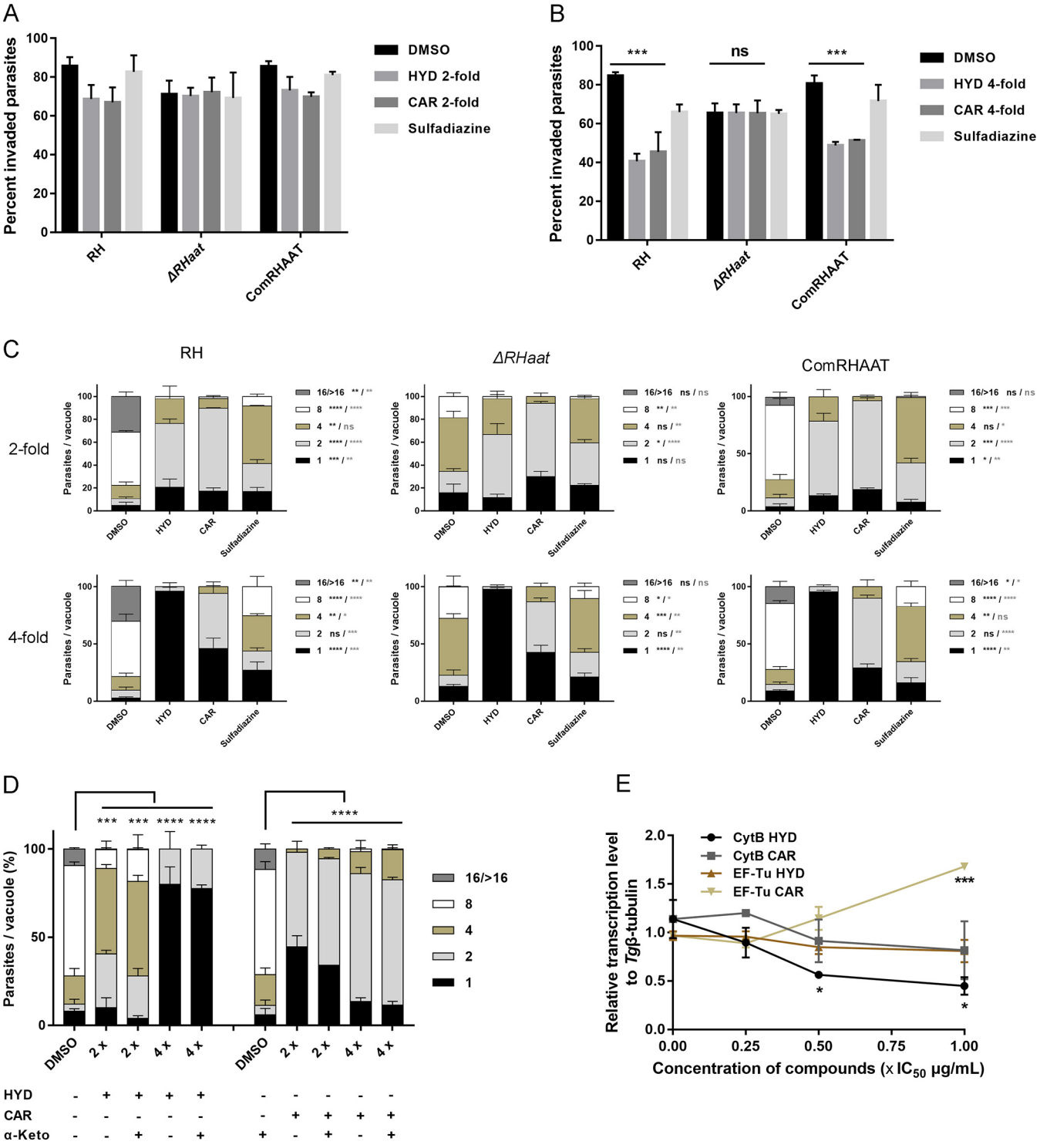

FIG 8 HYD and CAR inhibit *T. gondii* growth through an AAT-independent pathway. (A and B) Effects of AAT-deficient parasite invasion treated with HYD and CAR compared to parental and complemented. The data show the means ± the SEM of three independent experiments. ***, $P < 0.001$, determined by chi-square test. (C) Effects of HYD and CAR treatment for AAT-deficient parasite replication. The concentration of the 2- or 4-fold IC_{50} values of HYD and CAR were used to treat parasite replication by three strains. *, $P < 0.05$; **, $P < 0.01$; ***, $P < 0.001$; ****, $P < 0.0001$. A heavy asterisk stands for HYD versus vehicle, and a light asterisk stands for CAR versus vehicle, determined by Tukey's multiple-comparison test. (D) α-Ketoglutarate (α-Keto) assay. α-Ketoglutarate was supplemented to the HYD and CAR treatment medium, and then replication was determined at 24 h postinfection. ***, $P < 0.001$; ****, $P < 0.0001$, determined by Tukey's multiple-comparison test. (E) Effects of HYD and CAR on mitochondrial genome and apicoplast genome. A total of 2×10^7 tachyzoites were treated by 0.25-, 0.5-, and 1-fold IC_{50} values of HYD, CAR, or sulfadiazine (1 mg/ml) for 5 days to investigate the expression of CytB and the EF-Tu gene by qPCR. *, $P < 0.05$; ***, $P < 0.001$, one-way ANOVA plus Dunnett's multiple-comparison test.

examined the high selectivity indices of 49.04 and >43.27 against *T. gondii*, confirming that HYD and CAR should be safe and efficient at inhibiting the growth of *T. gondii*.

It has been reported that HYD and CAR inhibited AAT activity in *P. falciparum*, which is responsible for the reversible reaction of aspartate and α-ketoglutarate into oxaloacetate and glutamate (19, 22). In the present study, although the reaction of transamination of r*Tg*AAT, which catalyzes aspartate and α-ketoglutarate to glutamate, was inhibited by HYD and CAR treatments, >10-fold differences in the IC_{50} values of HYD or CAR against cultured type I *T. gondii* parasites versus r*Tg*RHAAT enzyme were recorded. This weakens the argument that these compounds inhibited *Toxoplasma* parasites by targeting AAT. Our findings are in contrast to a previous study on *P. falciparum* which determined a parasitic IC_{50} value in the same range that of HYD for the r*Pf*AAT enzyme *in vitro* (19). *Tg*AATs are distantly related to the predicted *P. falciparum* AATs, with a relatively low 33% identity; thus, it is possible that the AATs in two apicomplexan parasites have different functions, and different sites of drug action may occur. In a previous study, Berger et al. (22) found that AATs also play a role in the final step of methionine regeneration from methylthioadenosine in parasitic protozoa, but since this reaction is dependent on transamination, it was not investigated here.

As expected, our results confirm that deficiency of AAT both in RH and in PLK inhibited the parasite's ability to invade, replicate, egress, and form plaques *in vitro*, consistent with the inhibition of the *T. gondii* lytic cycle by HYD and CAR, although the loss of AAT did not completely abolish parasite growth. However, the intracellular replication of AAT-deficient parasites was inhibited by HYD or CAR similar to parental parasites. This suggests that another pathway might be the target of these compounds. HYD and CAR treatment did not significantly slow down the invasion rates of mutant parasites compared to parental parasites, which may imply that compounds have slight activity to inhibit invasion by AAT reaction, consistent with the current catalytic inhibitor assay. Collectively, HYD and CAR inhibit parasite growth largely through other substrates in *T. gondii*.

On the other hand, the growth defect due to loss of AAT was significantly rescued by treatment with α-ketoglutarate (400 μM). Interestingly, a high concentration (2 mM) of α-ketoglutarate led to faster intracellular replication of AAT-deficient parasites compared to parental PLK *in vitro*. This indicates that a loss of AAT in *T. gondii* impairs α-ketoglutarate homeostasis, which is related to parasite growth *in vitro*. This finding may also explain why a deficiency of AAT in PLK caused parasites to proliferate faster in mice (Fig. S3), since mice have higher metabolic α-ketoglutarate levels. High parasite burdens led to unexpected upregulation of cytokines and a lethal outcome, which is attributed to the enhanced virulence of PLK *in vivo* in accordance with previous investigations (30, 31). All of these findings indicate that although AAT is not essential for parasite growth under standard culture conditions, it plays a central role in the complex metabolic balance of α-ketoglutarate metabolism, which is largely involved in the carbon skeleton via glutamine metabolism, as in *P. falciparum* (1, 13, 19, 22, 32).

However, our data show that the impaired replication caused by HYD and CAR treatment was not rescued through α-ketoglutarate supplementation. These observations show that the inhibition activity of HYD and CAR may not be due to the association of the α-ketoglutarate mechanism to AAT or other metabolic enzymes of the α-ketoglutarate pathway (1, 13). In addition, this impairment of α-ketoglutarate homeostasis in *T. gondii* by a loss of AAT enhanced PLK parasitic virulence *in vivo*. Therefore, we doubt whether α-ketoglutarate reuptake affects the virulence of type II PLK parasites *in vivo*, and we assume that the metabolic enzymes directly related to α-ketoglutarate uptake may not be effective drug targets against *T. gondii*. Overall, our data suggest that the control of parasite growth by HYD and CAR is not a result of the inhibition of α-ketoglutarate pathway on *T. gondii in vitro* and *in vivo*.

In this study, the data showed that HYD and CAR control acute toxoplasmosis and inhibit *T. gondii* growth in mice but that AAT deficiency does not reduce the virulence

of *T. gondii in vivo*. Hence, HYD and CAR might be acting on *T. gondii* through a manner independent of the AAT pathway *in vivo*. Interestingly, these two compounds exhibited similar inhibitory activities in different tests, which may be because of the hydroxylamine unit in the structure of CAR. Hydroxylamine and its compounds have the potential to inhibit the activity of some enzymes in viruses, bacteria, fungi, and protozoa (33, 34). HYD and CAR impairment of the parasite lytic cycle may be associated with the inhibition of the mitochondrial function of the α-ketoglutarate-independent pathway (35, 36). However, further studies focusing on the elucidation of the mechanism of inhibition are warranted. Our study hints at new substrates of HYD and CAR as potential drug targets to inhibit *T. gondii* growth.

MATERIALS AND METHODS

Animals. Six-week-old female BALB/c mice were purchased from Clea Japan (Tokyo, Japan) for the preparation of polyclonal antibodies against *T. gondii*-specific proteins and for survival assays. Mice were housed in the animal facility of National Research Center for Protozoan Diseases, Obihiro University of Agriculture and Veterinary Medicine, with an adequate temperature (25 $\pm$ 2°C) and luminosity (12-h light, 12-h dark) under specific-pathogen-free conditions, with free access to food and water. All animal experiments started 1 week after habituation. The recommendations in the *Guide for the Care and Use of Laboratory Animals* of Obihiro University of Agriculture and Veterinary Medicine, Obihiro, Japan, were strictly followed. The protocol of the present study was approved by the Committee on the Ethics of Animal Experiments of Obihiro University of Agriculture and Veterinary Medicine (permissions 201711 and 2018728).

Parasite cultures. *T. gondii* RH strain (type I) with hypoxanthine-xanthine-guanine phosphoribosyl transferase (HXGPRT) deficiency, RH-GFP (a green fluorescent protein expressing-RH strain) (26), and PLK strain (type II) were used in this study. The parasites were maintained in monkey kidney adherent epithelial (Vero) cells cultured in Eagle minimum essential medium (EMEM; Sigma) supplemented with 8% fetal bovine serum (FBS; Biowest, Japan), as well as 100 U ml^{-1} penicillin and 100 mg ml^{-1} streptomycin (Sigma), at 37°C and 5% CO_2. Parasites were cultured in HFF cells maintained in Dulbecco modified Eagle medium (Sigma) supplemented with 10% FBS, 100 U ml^{-1} penicillin, and 100 mg ml^{-1} streptomycin at 37°C in a 5% CO_2 atmosphere. For the purification of tachyzoites, the parasites and host cells were washed with sterile PBS and peeled from the plate with a cell scraper (BD Bioscience). The final pellet was passed through a 27-gauge needle syringe three times, filtered through a 5.0-μm-pore filter (Millipore), and counted.

Chemicals. Hydroxylamine (HYD) and carboxymethoxylamine hemihydrochloride (CAR) were purchased from Sigma (catalog numbers 7803-49-8 and 86-08-8). The inhibitors were dissolved in double-distilled water and DMSO, respectively, and stored at –30°C until use.

Production of recombinant proteins and polyclonal antibodies. *Tg*AAT genes of the RH strain (*Toxoplasma* Genomics Resource TGGT1_248600) and the PLK strain (*Toxoplasma* Genomics Resource TGME49_248600) were amplified by PCR from *T. gondii* RH and PLK parasite cDNAs, respectively. The primers used included a SalI site (underlined) in the forward primer 5′-ACGC GTCGAC ATG TTT CCA ACT CTT AGT GAG AAC C-3′ and a NotI site (underlined) in the reverse primer 5′-ATAAGAAT GCGGCCGC TTA GCT TGC AGG AAC TGC CCG CAC CA-3′. PCR products digested with SalI and NotI were inserted into a pGEX-4T-1 plasmid vector treated with the same restriction enzymes (Roche, Switzerland). The fragments were sequenced using a BigDye terminator cycle sequencing kit (Applied Biosystems) and an ABI Prism 3100 genetic analyzer (Applied Biosystems). pGEX-4T-3-SAG1 (37) and pGEX-4T-3-GRA7 (38) plasmids from previous studies were used to produce recombinant *Tg*SAG1-GST and *Tg*GRA7-GST proteins. Recombinant pGEX-4T-1-AAT, pGEX-4T-3-SAG1, and pGEX-4T-3-GRA7 were expressed as glutathione *S*-transferase (GST) fusion protein in *Escherichia coli* BL21(DE3) (New England BioLabs, Inc.) and purified with glutathione-Sepharose 4B beads (GE Healthcare Life Sciences) according to the manufacturer's instructions. Purified recombinant protein *Tg*AAT-GST (100 μg) and *Tg*SAG1-GST (100 μg) emulsified in Freund complete adjuvant (Sigma) were i.p. injected into BALB/c mice to produce mouse anti-*Tg*AAT and anti-*Tg*SAG1 polyclonal antibodies. Purified recombinant proteins *Tg*SAG1-GST (1 mg) and *Tg*GRA7-GST (1 mg) were subcutaneously injected into female Japanese white rabbits to produce rabbit anti-*Tg*SAG1 and anti-*Tg*GRA7 polyclonal antibodies.

Cytotoxicity analysis of HYD and CAR on HFF and Vero cells. Cytotoxicity of the two compounds were determined both on HFF and Vero cells using a Cell Counting Kit-8 (CCK-8; Dojindo Molecular Technologies, Inc., Japan) according to the manufacturer's instructions. Briefly, the cells were plated in 96-well plates at densities of 1×10^4 (HFFs) or 1×10^5 (Vero cells) per well and then incubated for 48 h (HFF cells) or 24 h (Vero cells) at 37°C in a 5% CO_2 atmosphere. The cells were then exposed to the compounds at final concentrations of 1, 5, 10, 25, 50, 100, 200, 400, 800, or 1,000 μg/ml for 24 h, with CCK-8 reagent added and reacted for 4 h. The absorbance of the supernatant was measured at 450 nm using an MTP-120 microplate reader (Corona Electric, Ibaraki, Japan). Cell viability (%) was calculated in three independent experiments.

Inhibition assay of HYD and CAR on *Toxoplasma in vitro*. To evaluate anti-*Toxoplasma* potential *in vitro*, a growth inhibition assay was performed with the two inhibitors and sulfadiazine (Sigma-Aldrich). Purified RH-GFP tachyzoites at 5×10^4/well were used and added to 96-well plates, where HFF cells were seeded (1×10^4 cells/well) and cultured for 48 h. After 4 h, the extracellular parasites were washed out. The compounds—at final concentrations of 1, 3.125, 6.25, 12.5, 25, or 50 μg/ml in HYD cultures or 1, 5,

10, 15, 20, 25, 50, or 100 μg/ml in CAR cultures—were added. Medium and sulfadiazine (1 mg/ml) were used as negative and positive controls, respectively. The fluorescence intensity of RH-GFP was measured using a microplate reader (SH-900; Corona Electric Co., Ltd., Ibaraki, Japan) after 72 h of incubation. Each concentration was determined in three independent experiments together to calculate the half-maximal inhibitory concentration (IC_{50}) values on *T. gondii* using Prism 7 software (GraphPad Software, Inc., La Jolla, CA).

Growth assays on extracellular and intracellular *T. gondii in vitro*. To examine the effects of compounds on parasite growth, 2- or 4-fold final concentrations (IC_{50}) of compounds, DMSO, and sulfadiazine (1 mg/ml) were used to perform plaque formation, extracellular invasion, intracellular replication, and egress assays on RH and PLK strain parasites as follows. All assays were conducted in triplicate and repeated at least three times.

For the plaque assays, fresh purified tachyzoites (150 of RH and 300 of PLK per well) were inoculated onto monolayers of Vero cells or HFFs in 12-well plate and grown for 8 days for RH parasites and 12 days for PLK parasites at 37°C in 5% CO_2. Subsequently, the samples were fixed with 4% paraformaldehyde, stained with 0.1% crystal violet, and imaged on a scanner to analyze the number and relative sizes of plaques, as described previously (24). For the compound assay, at 2 h after parasite infection, the old medium was replaced by the new medium with 2- or 4-fold IC_{50}s of compounds and DMSO, followed by culture for 8 days.

The invasion assay was performed using the indirect fluorescent antibody test (IFAT) (39). Vero cells (1×10^5 per well) were used to plate on 12-well cultured for 24 h. Fresh purified tachyzoites (2×10^5 per well) were inoculated onto cell monolayers for 2 h infection under normal growth conditions. For the compound assay, tachyzoites (2×10^5) were pretreated with either of the two compounds at 2- or 4-fold IC_{50}s, sulfadiazine (1 mg/ml), or DMSO for 1 h at 37°C and then cultured for 2 h. The coverslips were washed with PBS six times to remove extracellular parasites and fixed. Mouse anti-SAG1 polyclonal antibody diluted 1:500 and Alexa Fluor 594-conjugated goat anti-mouse IgG (Sigma) diluted 1:1,000 were then used to count the numbers of attached parasites. After permeabilization with 0.3% Triton X-100/PBS, rabbit anti-SAG1 polyclonal antibody diluted 1:500 and Alexa Fluor 488-conjugated goat anti-rabbit IgG (Sigma) were used to count the numbers of invading parasites, as described previously (3). Samples were examined using an All-in-One fluorescence microscope (BZ-900; Keyence, Japan). Cells that were stained both red and green were scored as attached parasites, whereas those that were stained only in green were scored as invaded parasites. Ten fields were randomly counted for each coverslip.

For the intracellular replication assay, the intracellular replication rate was evaluated by counting the numbers of parasites per vacuole, as previously described (39). Vero cells (1×10^5 per well) were used to plate on 12-well plates cultured for 24 h. Fresh purified tachyzoites (2×10^5 per well) were inoculated onto cell monolayers for 2 h of infection under normal growth conditions. Every well was washed with PBS six times to remove extracellular parasites and then cultured for 24 or 32 h. To examine compound effects on replication, at 2 h postinfection under standard growth conditions the new medium with a 2- or a 4-fold IC_{50} of compounds was added to cell well, followed by culture for 24 h. Tachyzoites in vacuoles were marked with mouse anti-SAG1 by IFAT at 24 or 32 h postinfection as described above and counted in at least 100 vacuoles.

For the egress assay, Vero cells (1×10^5 per well) were used to plate on 12-well cultured for 24 h. Fresh purified tachyzoites (2×10^5 per well) were inoculated onto cell monolayers for 32 h of infection under normal growth conditions, as previously described (3). The wells were washed with PBS five times to remove extracellular parasites and then incubated with 3 μM A23187 (Sigma). For the HYD and CAR assays, infected cells were treated by 2- and 4-fold IC_{50}s of compounds for 10 min before incubation with 3 μM A23187. After incubation, the cells were fixed, and the IFAT was performed with mouse anti-SAG1 and rabbit anti-GRA7 to measure the percentages of egressed parasitophorous vacuoles (PVs). At least 300 vacuoles were counted per slip.

Virulence tests in mouse model. Fresh tachyzoites were purified and counted as described above and then used to inject 7-week-old female BALB/c mice by i.p. injection. For treatment in the HYD and CAR assays, at 24 h postinfection, acutely infected mice were i.p. injected with the compounds (5 or 20 mg/kg HYD; 10, 25, and 50 mg/kg CAR; or PBS) for 7 days. Daily observations, such as body weight, morbidity, mortality, and clinical signs, were noted, as were the clinical scores (7). Surviving mice were monitored for 30 days, and blood was drawn at day 30 to confirm infection using an enzyme-linked immunosorbent assay; tissues were collected to determine parasite burdens through targeting of the *Tg*B1 gene by qPCR. GraphPad Prism 7 was used to graph cumulative mortality as Kaplan-Meier survival plots, and the results were analyzed.

Enzyme activity assay. Enzyme-coupled assays were performed as described previously (19). The concentration of soluble r*Tg*AAT-fused GST was determined to be 1 μg, which was used to perform an enzyme-coupled assay with the specific substrates L-aspartate and α-ketoglutarate (Sigma). The basic reaction principle is that L-aspartate and α-ketoglutarate were catalyzed to glutamate by r*Tg*AAT, and then glutamate with 3-acetylpyridine adenine dinucleotide (APAD; Sigma) are converted to APADH by glutamate dehydrogenase (Sigma); the absorbance of the supernatant was determined at 363 nm. Two reported specific enzymatic inhibitors, including HYD and CAR (Sigma), were used to perform the inhibitor assay (19). All experiments were tested three times independently.

Generation of possible HYD and CAR targeting gene AAT-knockout and complemented lines on RH and PLK strains. All the primers used in this study are listed in Table S1 in the supplemental material. The *T. gondii* aspartate aminotransferase-targeting guide RNA (gRNA) sequence was designed using E-CRISP (E-Crisp.org). The *Tg*AAT-specific CRISPR knockout plasmids (pDF-Cas9-sgRH/PLKAAT, Fig. S2D) containing Cas9, GFP, guide RNA, and dihydrofolate reductase DHFR expression cassettes were generated by replacing

the original targeting gRNA in pDF-PLK-GRA9 plasmid (3). RH and PLK parasites (10^7 tachyzoites) were transfected with 10 μg of the pDF-Cas9-sgRH/PLKAAT plasmids, respectively, as previously described (40). Selection of stable transformants based on pyrimethamine (1 μM) was performed as described previously (41, 42). Stable knockout lines (Δ*RHaat* and Δ*PLKaat* strains) were isolated by limiting dilution in 96-well plates and confirmed by PCR, Western blotting (WB), and IFAT.

The full *Tg*AAT fragment containing synonymous codons mutated at target sites for gRNA was amplified from RH and PLK cDNA by overlap PCR to generate the complemented AAT plasmids (pB-synoRHAAT and pB-synoPLKAAT), respectively. The Δ*RHaat* and Δ*PLKaat* parasites (10^7 tachyzoites) were transfected with pHX-UPRT and linearized pB-synoRHAAT or pB-synoPLKAAT by SacI (mass ratio, 1:5; Roche, Switzerland) to generate complemented strains (ComRHAAT and ComPLKAAT strains) by insertion at the UPRT locus, as described previously (3). Parasites were screened with 10 μM 5-fluorouracil (Sigma). Positive clones were confirmed as described above. All of the plasmids were verified by DNA sequencing before use.

Examination of parasite growth during AAT deficiency *in vitro* and *in vivo*. To determine the effect on parasite growth after loss of AAT on RH and PLK strains, all strain parasites, including wild-type, Δ*aat*, and ComAAT strains, were used to perform plaque formation, extracellular invasion, intracellular replication, and egress assays *in vitro*, as well as a virulence assay *in vivo*, as described above. All experiments were conducted in triplicate and repeated at least three times.

Metabolic treatment assay of Δ*aat* strains *in vitro*. For the metabolic treatment assay, α-ketoglutarate is dissolved in EMEM supplemented with 8% FBS, 100 U ml^{-1} penicillin, and 100 mg ml^{-1} streptomycin to a final concentration of 400 μM or 2 mM. The parasites were maintained in Vero cells in EMEM containing α-ketoglutarate or normal EMEM to perform an intracellular replication assay at 24 or 32 h postinfection and a plaque assay as described above, respectively. Subsequently, different phenotypes were recorded and analyzed.

Growth examination of treatment with HYD and CAR on extracellular and intracellular AAT-deficient parasites *in vitro*. To determine whether HYD and CAR specifically targets *Toxoplasma* AAT protein, 2- or 4-fold IC_{50} values of the compounds and sulfadiazine were used to develop extracellular invasion and intracellular replication assays for RH, Δ*RHaat*, and ComRHAAT strains, as described above. In addition, parasite replication was examined during exposure to 2- or 4-fold of IC_{50}s of two compounds and 400 μM α-ketoglutarate.

DNA isolation and quantitative PCR detection of *T. gondii*. DNA was extracted from the brains of HYD-, CAR-, or PBS-treated surviving mice on day 30 by using a DNeasy Blood & Tissue kit (Qiagen, Germany) according to the manufacturer's instructions. The brain DNA was then amplified with specific primers targeting to the *T. gondii* B1 gene (forward primer 5′-AAC GGG CGA GTA GCA CCT GAG GAG-3′ and reverse primer 5′-TGG GTC TAC GTC GAT GGC ATG ACA AC-3′) by qPCR. A standard curve was constructed using 10-fold serial dilutions of *T. gondii* DNA extracted from 10^5 parasites; thus, the curve ranged from 0.01 to 10,000 parasites. The parasite number was calculated from the standard curve. Likewise, DNA was extracted from 2×10^7 tachyzoites treated with 0.25-, 0.5-, or 1-fold IC_{50} values of HYD and CAR or sulfadiazine (1 mg/ml). DNA from each tachyzoite sample (30 ng) treated with 1/4, 1/2, and IC_{50} concentrations of HYD and CAR were used to amplify fragments of *Toxoplasma* mitochondrial genome cytochrome *b* (CytB) (forward primer 5′-TAC CGC TTG GAT GTC TGG TT-3′ and reverse primer 5′-AAC CTC CAA GTA GCC AAG GT-3′) and apicoplast genome elongation factor Tu (EF-Tu; using forward primer 5′-TGT GCT CCT GAA GAA ATA GC-3′ and reverse primer 5′-CAT TGG CCC ATC TAC AGC AG-3′), respectively, as previously described (33, 34). The expression levels of target genes were normalized to *Tg* β-tubulin (forward primer 5′-CAC TGG TAC ACG GGT GAA GGT-3′ and reverse primer 5′-ATT CTC CCT CTT CCT CTG CG-3′) mRNA levels using the $2^{\Delta\Delta CT}$ method.

The amplification was performed with DNA, 1× PowerUp SYBR Green Master Mix (Thermo Fisher Scientific, Inc., Waltham, MA), and 500 nM concentrations of gene-specific primers in a 10-μl total reaction volume using a standard protocol recommended by the manufacturer (2 min at 50°C, 10 min at 95°C, and then 40 cycles of 95°C for 15 s and 60°C for 1 min). Amplification, data acquisition, and data analysis were carried out using the ABI Prism 7900HT sequence detection system (Applied Biosystems), and the cycle threshold values (C_T) were calculated as described previously (43).

Statistical analysis. To graph and analyze the data, we used Prism 7 software. Statistical analyses were performed with an unpaired Student *t* test, the Tukey's multiple-comparison test, a chi-square test, and one-way analysis of variance (ANOVA) plus Tukey-Kramer *post hoc* analysis. The data represent means ± standard errors of mean (SEM). Survival curves were generated using the Kaplan-Meier method, and statistical comparisons were made by the log-rank method. A *P* value of <0.05 was considered statistically significant.

SUPPLEMENTAL MATERIAL

Supplemental material is available online only.

SUPPLEMENTAL FILE S1, PDF file, 0.8 MB.

ACKNOWLEDGMENTS

This study was supported by grants from Japan Society for the Promotion of Science Core-to-Core Program.

We declare that we have no competing interests.

REFERENCES

1. Jacot D, Waller RF, Soldati-Favre D, MacPherson DA, MacRae JI. 2016. Apicomplexan energy metabolism: carbon source promiscuity and the quiescence hyperbole. Trends Parasitol 32:56–70. https://doi.org/10.1016/j.pt.2015.09.001.
2. Weiss LM, Dubey JP. 2009. Toxoplasmosis: a history of clinical observations. Int J Parasitol 9:895–901. https://doi.org/10.1016/j.ijpara.2009.02.004.
3. Guo H, Gao Y, Jia H, Moumouni PFA, Masatani T, Liu M, Lee SH, Galon EM, Li J, Li Y, Tumwebaze MA, Benedicto B, Xuan X. 2019. Characterization of strain-specific phenotypes associated with knockout of dense granule protein 9 in *Toxoplasma gondii*. Mol Biochem Parasitol 229:53–61. https://doi.org/10.1016/j.molbiopara.2019.01.003.
4. Howe DK, Sibley LD. 1995. *Toxoplasma gondii* comprises three clonal lineages: correlation of parasite genotype with human disease. J Infect Dis 172:1561–1566. https://doi.org/10.1093/infdis/172.6.1561.
5. Sibley LD, Ajioka JW. 2008. Population structure of *Toxoplasma gondii*: clonal expansion driven by infrequent recombination and selective sweeps. Annu Rev Microbiol 62:329–351. https://doi.org/10.1146/annurev.micro.62.081307.162925.
6. Halonen SK, Weiss LM. 2013. Toxoplasmosis. Handb Clin Neurol 114:125–145. https://doi.org/10.1016/B978-0-444-53490-3.00008-X.
7. Leesombun A, Boonmasawai S, Shimoda N, Nishikawa Y. 2016. Effects of extracts from Thai *Piperaceae* plants against infection with *Toxoplasma gondii*. PLoS One 11:e0156116. https://doi.org/10.1371/journal.pone.0156116.
8. Wei HX, Wei SS, Lindsay DS, Peng HJ. 2015. A systematic review and meta-analysis of the efficacy of anti-*Toxoplasma gondii* medicines in humans. PLoS One 10:e0138204. https://doi.org/10.1371/journal.pone.0138204.
9. Scheele S, Geiger JA, DeRocher AE, Choi R, Smith TR, Hulverson MA, Vidadala RSR, Barrett LK, Maly DJ, Merritt EA, Ojo KK, Van Voorhis WC, Parsons M. 2018. Toxoplasma calcium-dependent protein kinase 1 inhibitors: probing activity and resistance using cellular thermal shift assays. Antimicrob Agents Chemother 62:e00051-18. https://doi.org/10.1128/AAC.00051-18.
10. Nitzsche R, Zagoriy V, Lucius R, Gupta N. 2016. Metabolic cooperation of glucose and glutamine is essential for the lytic cycle of obligate intracellular parasite *Toxoplasma gondii*. J Biol Chem 291:126–141. https://doi.org/10.1074/jbc.M114.624619.
11. Fleige T, Fischer K, Ferguson DJ, Gross U, Bohne W. 2007. Carbohydrate metabolism in the *Toxoplasma gondii* apicoplast: localization of three glycolytic isoenzymes, the single pyruvate dehydrogenase complex, and a plastid phosphate translocator. Eukaryot Cell 6:984–996. https://doi.org/10.1128/EC.00061-07.
12. Fleige T, Pfaff N, Gross U, Bohne W. 2008. Localization of gluconeogenesis and tricarboxylic acid (TCA) cycle enzymes and first functional analysis of the TCA cycle in *Toxoplasma gondii*. Int J Parasitol 38:1121–1132. https://doi.org/10.1016/j.ijpara.2008.01.007.
13. MacRae JI, Sheiner L, Nahid A, Tonkin C, Striepen B, McConville MJ. 2012. Mitochondrial metabolism of glucose and glutamine is required for intracellular growth of *Toxoplasma gondii*. Cell Host Microbe 12:682–692. https://doi.org/10.1016/j.chom.2012.09.013.
14. Blume M, Nitzsche R, Sternberg U, Gerlic M, Masters SL, Gupta N, McConville MJ. 2015. A *Toxoplasma gondii* gluconeogenic enzyme contributes to robust central carbon metabolism and is essential for replication and virulence. Cell Host Microbe 18:210–220. https://doi.org/10.1016/j.chom.2015.07.008.
15. Oppenheim RD, Creek DJ, Macrae JI, Modrzynska KK, Pino P, Limenitakis J, Polonais V, Seeber F, Barrett MP, Billker O, McConville MJ, Soldati-Favre D. 2014. BCKDH: the missing link in apicomplexan mitochondrial metabolism is required for full virulence of *Toxoplasma gondii* and *Plasmodium berghei*. PLoS Pathog 10:e1004263. https://doi.org/10.1371/journal.ppat.1004263.
16. Zheng J, Jia H, Zheng Y. 2015. Knockout of leucine aminopeptidase in *Toxoplasma gondii* using CRISPR/Cas9. Int J Parasitol 45:141–148. https://doi.org/10.1016/j.ijpara.2014.09.003.
17. Xia N, Yang J, Ye S, Zhang L, Zhou Y, Zhao J, David Sibley L, Shen B. 2018. Functional analysis of *Toxoplasma* lactate dehydrogenases suggests critical roles of lactate fermentation for parasite growth *in vivo*. Cell Microbiol 20:e12794. https://doi.org/10.1111/cmi.12794.
18. Xia N, Ye S, Liang X, Chen P, Zhou Y, Fang R, Zhao J, Gupta N, Yang S, Yuan J, Shen B. 2019. Pyruvate homeostasis as a determinant of parasite growth and metabolic plasticity in *Toxoplasma gondii*. mBio 10:e00898-19. https://doi.org/10.1128/mBio.00898-19.
19. Wrenger C, Müller IB, Schifferdecker AJ, Jain R, Jordanova R, Groves MR. 2011. Specific inhibition of the aspartate aminotransferase of *Plasmodium falciparum*. J Mol Biol 405:956–971. https://doi.org/10.1016/j.jmb.2010.11.018.
20. Wrenger C, Muller IB, Silber AM, Jordanova R, Lamzin VS, Groves MR. 2012. Aspartate aminotransferase: bridging carbohydrate and energy metabolism in *Plasmodium falciparum*. Curr Drug Metab 13:332–336. https://doi.org/10.2174/138920012799320400.
21. Marković-Housley Z, Schirmer T, Hohenester E, Khomutov AR, Khomutov RM, Karpeisky MY, Sandmeier E, Christen P, Jansonius JN. 1996. Crystal structures and solution studies of oxime adducts of mitochondrial aspartate aminotransferase. Eur J Biochem 236:1025–1032. https://doi.org/10.1111/j.1432-1033.1996.01025.x.
22. Berger LC, Wilson J, Wood P, Berger BJ. 2001. Methionine regeneration and aspartate aminotransferase in parasitic protozoa. J Bacteriol 183:4421–4434. https://doi.org/10.1128/JB.183.15.4421-4434.2001.
23. Lourido S, Tang K, Sibley LD. 2012. Distinct signaling pathways control *Toxoplasma* egress and host-cell invasion. EMBO J 31:4524–4534. https://doi.org/10.1038/emboj.2012.299.
24. Shen B, Sibley LD. 2014. Toxoplasma aldolase is required for metabolism but dispensable for host-cell invasion. Proc Natl Acad Sci U S A 111:3567–3572. https://doi.org/10.1073/pnas.1315156111.
25. de Oliveira TC, Silva DA, Rostkowska C, Béla SR, Ferro EA, Magalhães PM, Mineo JR. 2009. *Toxoplasma gondii*: effects of *Artemisia annua* L. on susceptibility to infection in experimental models *in vitro* and *in vivo*. Exp Parasitol 122:233–241. https://doi.org/10.1016/j.exppara.2009.04.010.
26. Nishikawa Y, Xuenan X, Makala L, Vielemeyer O, Joiner KA, Nagasawa H. 2003. Characterization of *Toxoplasma gondii* engineered to express mouse interferon-gamma. Int J Parasitol 33:1525–1535. https://doi.org/10.1016/s0020-7519(03)00204-2.
27. Nishikawa Y, Zhang H, Ibrahim HM, Ui F, Ogiso A, Xuan X. 2008. Construction of *Toxoplasma gondii* bradyzoite expressing the green fluorescent protein. Parasitol Int 57:219–222. https://doi.org/10.1016/j.parint.2007.10.004.
28. Leesombun A, Iijima M, Umeda K, Kondoh D, Pagmadulam B, Abdou AM, Suzuki Y, Ohba SI, Isshiki K, Kimura T, Kubota Y, Sawa R, Nihei CI, Nishikawa Y. 2019. Metacytofilin is a potent therapeutic drug candidate for toxoplasmosis. J Infect Dis 2019:jiz501.
29. Abugri DA, Witola WH, Russell AE, Troy RM. 2018. *In vitro* activity of the interaction between taxifolin (dihydroquercetin) and pyrimethamine against *Toxoplasma gondii*. Chem Biol Drug Des 91:194–201. https://doi.org/10.1111/cbdd.13070.
30. Suzuki Y, Orellana MA, Schreiber RD, Remington JS. 1988. Interferon-gamma: the major mediator of resistance against *Toxoplasma gondii*. Science 240:516–518. https://doi.org/10.1126/science.3128869.
31. Mordue DG, Monroy F, La Regina M, Dinarello CA, Sibley LD. 2001. Acute toxoplasmosis leads to lethal overproduction of Th1 cytokines. J Immunol 167:4574–4584. https://doi.org/10.4049/jimmunol.167.8.4574.
32. Jain R, Jordanova R, Müller IB, Wrenger C, Groves MR. 2010. Purification, crystallization, and preliminary X-ray analysis of the aspartate aminotransferase of *Plasmodium falciparum*. Acta Crystallogr Sect F Struct Biol Cryst Commun 66:409–412. https://doi.org/10.1107/S1744309110003933.
33. Gross P. 1985. Biologic activity of hydroxylamine: a review. Crit Rev Toxicol 14:87–99. https://doi.org/10.3109/10408448509023765.
34. Sarojini G, Oliver DJ. 1985. Inhibition of glycine oxidation by carboxymethoxylamine, methoxylamine, and acethydrazide. Plant Physiol 77:786–789. https://doi.org/10.1104/pp.77.3.786.
35. Uddin T, McFadden GI, Goodman CD, Uddin T, McFadden GI, Goodman CD. 2018. Validation of putative apicoplast-targeting drugs using a chemical supplementation assay in cultured human malaria parasites. Antimicrob Agents Chemother 62:e01161-17. https://doi.org/10.1128/AAC.01161-17.
36. Korsinczky M, Chen N, Kotecka B, Saul A, Rieckmann K, Cheng Q. 2000. Mutations in *Plasmodium falciparum* cytochrome *b* that are associated with atovaquone resistance are located at a putative drug-binding site. Antimicrob Agents Chemother 44:2100–2108. https://doi.org/10.1128/aac.44.8.2100-2108.2000.
37. Kimbita EN, Xuan X, Huang X, Miyazawa T, Fukumoto S, Mishima M,

Suzuki H, Sugimoto C, Nagasawa H, Fujisaki K, Suzuki N, Mikami T, Igarashi I. 2001. Serodiagnosis of *Toxoplasma gondii* infection in cats by enzyme-linked immunosorbent assay using recombinant SAG1. Vet Parasitol 102:35–44. https://doi.org/10.1016/s0304-4017(01)00522-2.

38. Masatani T, Matsuo T, Tanaka T, Terkawi MA, Lee EG, Goo YK, Aboge GO, Yamagishi J, Hayashi K, Kameyama K, Cao S, Nishikawa Y, Xuan X. 2013. TgGRA23, a novel *Toxoplasma gondii* dense granule protein associated with the parasitophorous vacuole membrane and intravacuolar network. Parasitol Int 62:372–379. https://doi.org/10.1016/j.parint.2013.04.003.
39. Wang M, Cao S, Du N, Fu J, Li Z, Jia H, Song M. 2017. The moving junction protein RON4, although not critical, facilitates host cell invasion and stabilizes MJ members. Parasitology 144:1490–1497. https://doi.org/10.1017/S0031182017000968.
40. Soldati D, Boothroyd JC. 1993. Transient transfection and expression in the obligate intracellular parasite *Toxoplasma gondii*. Science 260:349–352. https://doi.org/10.1126/science.8469986.
41. Donald RG, Roos DS. 1998. Gene knock-outs and allelic replacements in *Toxoplasma gondii*: HXGPRT as a selectable marker for hit-and-run mutagenesis. Mol Biochem Parasitol 91:295–305. https://doi.org/10.1016/s0166-6851(97)00210-7.
42. Reynolds MG, Oh J, Roos DS. 2001. *In vitro* generation of novel pyrimethamine resistance mutations in the *Toxoplasma gondii* dihydrofolate reductase. Antimicrob Agents Chemother 45:1271–1277. https://doi.org/10.1128/AAC.45.4.1271-1277.2001.
43. Mahmoud ME, Ui F, Salman D, Nishimura M, Nishikawa Y. 2015. Mechanisms of interferon-beta-induced inhibition of *Toxoplasma gondii* growth in murine macrophages and embryonic fibroblasts: role of immunity-related GTPase M1. Cell Microbiol 17:1069–1083. https://doi.org/10.1111/cmi.12423.